RAA 2015 Vol. **15** No. **11**, 1857–1866 doi: 10.1088/1674–4527/15/11/008
http://www.raa-journal.org *http://www.iop.org/journals/raa*

Research in Astronomy and Astrophysics

A first-order dynamical model of hierarchical triple stars and its application

Xing-Bo Xu[1,2], Fang Xia[1] and Yan-Ning Fu[1]

[1] Purple Mountain Observatory, Chinese Academy of Sciences, Nanjing 210008, China; *xbxu@pmo.ac.cn*
[2] University of Chinese Academy of Sciences, Beijing 100049, China

Received 2015 April 13; accepted 2015 May 15

Abstract For most hierarchical triple stars, the classical double two-body model of zeroth-order cannot describe the motions of the components under the current observational accuracy. In this paper, Marchal's first-order analytical solution is implemented and a more efficient simplified version is applied to real triple stars. The results show that, for most triple stars, the proposed first-order model is preferable to the zeroth-order model both in fitting observational data and in predicting component positions.

Key words: celestial mechanics — binaries: general — stars: kinematics and dynamics — methods: analytical

1 INTRODUCTION

A hierarchical triple star is composed of a close binary and a distant third component. About one thousand stars of this kind are contained in the latest on-line version of *The Multiple Star Catalog* (Tokovinin 1997). In these systems, the primary components are usually bright. Bright stars are useful in many aspects (e.g. Urban & Seidelmann 2014). Though a set of isotropic and dense stars is crucial for some applications such as navigation, the stars with nearby companions are usually excluded. This is the case for the Hipparcos Celestial Reference Frame, as recommended in IAU resolution B1 (2000)[1]. For triple stars, the problem lies mainly in that the primary positions generally cannot be predicted accurately by the almost exclusively used model, namely the classical double two-body model.

Hierarchical triple stars are also of great interest in stellar physics and galactic astronomy, due to the fact that their dynamical evolution is important to both stellar and galactic evolutions (e.g. Binney & Merrifield 1998; Valtonen & Karttunen 2006; Aarseth 2003). Moreover, these systems are often studied in terms of stability of the general three-body problem (e.g. Marchal & Bozis 1982; Li et al. 2009). In some case studies, the results are sensitive to the mass parameters and the initial conditions (e.g. Orlov & Zhuchkov 2005), the accuracies of which are limited again by the double two-body model used in fitting observations (e.g. Liu et al. 2009).

As a zeroth-order solution of the hierarchical three-body problem, the double two-body model has the advantage of being analytical and simple. The existing first-order analytical solutions are

[1] *http://www.iau.org/static/resolutions/IAU2000_French.pdf*

more accurate. The former one is still dominantly used, while the latter ones, as far as we know, remain little used in fitting observations. In this paper, the first-order solution by Marchal is efficiently implemented. This is achieved mainly by making some simplified modifications and high order approximations to Marchal's solution. In the context of fitting observations of triple stars, we call Marchal's solution and the double two-body solution, respectively, the M-model and the K-model.

In Section 2, the M-model is implemented. In Section 3, the improvement in accuracy from the M-model to the K-model is statistically discussed with a sample of triple stars. In Section 4, a simplified M-model is given and applied to real triple stars. Concluding remarks are given in the last section.

2 AN IMPLEMENTATION OF M-MODEL

Consider a hierarchical three-body problem in an inertial coordinate system $\{\mathrm{O}-xyz\}$, where O is the center of mass and the z-axis is parallel to the total angular momentum $\boldsymbol{C}$. Denoting the masses of the inner two bodies by m_1 and m_2, and the mass of the third body by m_3, we will use the following mass-dependent parameters,

$$m_t = m_1 + m_2 + m_3, \quad m_{\rm i} = \tfrac{m_1 m_2}{m_1+m_2}, \quad m_{\rm o} = \tfrac{(m_1+m_2)m_3}{m_t},$$
$$\beta_{\rm i} = \tfrac{G^2 m_1^3 m_2^3}{m_1+m_2}, \quad \beta_{\rm o} = \tfrac{G^2(m_1+m_2)^3 m_3^3}{m_t}, \quad \beta_1 = \tfrac{G^2(m_1+m_2)^7 m_3^7}{(m_1 m_2 m_t)^3},$$

where G is the gravitational constant. Let $\boldsymbol{r}$ be the position vector of m_2 relative to m_1, and $\boldsymbol{R}$ the position vector of m_3 relative to the center of mass of the binary. The ratio $\varepsilon = \frac{r}{R} \equiv \frac{|\boldsymbol{r}|}{|\boldsymbol{R}|}$ is a small quantity.

The Delaunay variables as expressed in terms of the ordinary orbital elements $(a, e, i, \Omega, \omega, M)$ are

$$\begin{array}{llllll}
\mathcal{L}_{\rm i} &= m_{\rm i}\sqrt{G(m_1+m_2)a_{\rm i}}\,, & \mathcal{G}_{\rm i} &= \mathcal{L}_{\rm i}\sqrt{1-e_{\rm i}^2}\,, & \mathcal{H}_{\rm i} &= \mathcal{G}_{\rm i}\cos i_{\rm i}\,, \\
\ell_{\rm i} &= M_{\rm i}\,, & g_{\rm i} &= \omega_{\rm i}\,, & h_{\rm i} &= \Omega_{\rm i}\,, \\
\mathcal{L}_{\rm o} &= m_{\rm o}\sqrt{G m_t a_{\rm o}}\,, & \mathcal{G}_{\rm o} &= \mathcal{L}_{\rm o}\sqrt{1-e_{\rm o}^2}\,, & \mathcal{H}_{\rm o} &= \mathcal{G}_{\rm o}\cos i_{\rm o}\,, \\
\ell_{\rm o} &= M_{\rm o}\,, & g_{\rm o} &= \omega_{\rm o}\,, & h_{\rm o} &= \Omega_{\rm o}\,,
\end{array}$$

where the subscripts "i" and "o" indicate the inner and outer orbits, respectively in these variables. The Hamiltonian up to the first order in $\varepsilon^2 \sim (\frac{\mathcal{L}_{\rm i}}{\mathcal{L}_{\rm o}})^4$ can be formally written as

$$\begin{aligned}
H &= H(\mathcal{L}_{\rm i}, \mathcal{G}_{\rm i}, \mathcal{L}_{\rm o}, \mathcal{G}_{\rm o}, \ell_{\rm i}, g_{\rm i}, \ell_{\rm o}, g_{\rm o}, \mathcal{H}_{\rm i}+\mathcal{H}_{\rm o}, h_{\rm o}-h_{\rm i}) \\
&\approx H_{0{\rm i}} + H_{0{\rm o}} + H_1 \\
&\equiv -\frac{\beta_{\rm i}}{2\mathcal{L}_{\rm i}^2} - \frac{\beta_{\rm o}}{2\mathcal{L}_{\rm o}^2} + \frac{\beta_1}{2\mathcal{L}_{\rm o}^2}\frac{(1-e_{\rm i}\cos E_{\rm i})^2}{(1-e_{\rm o}\cos E_{\rm o})^3}\left(1-3\Phi^2\right)\left(\frac{\mathcal{L}_{\rm i}}{\mathcal{L}_{\rm o}}\right)^4, \qquad (1)
\end{aligned}$$

where $\Phi = \Phi(\mathcal{L}_{\rm i}, \mathcal{G}_{\rm i}, \mathcal{L}_{\rm o}, \mathcal{G}_{\rm o}, \ell_{\rm i}, g_{\rm i}, \ell_{\rm o}, g_{\rm o}, \mathcal{H}_{\rm i}+\mathcal{H}_{\rm o}, h_{\rm o}-h_{\rm i}) = \frac{\boldsymbol{r}\cdot\boldsymbol{R}}{rR}$, and $E_{\rm i} = E_{\rm i}(\mathcal{L}_{\rm i}, \mathcal{G}_{\rm i}; \ell_{\rm i})$ and $E_{\rm o} = E_{\rm o}(\mathcal{L}_{\rm o}, \mathcal{G}_{\rm o}; \ell_{\rm o})$ are the eccentric anomalies of the inner and outer orbits, respectively.

In Equation (1), $\mathcal{H}_{\rm o}+\mathcal{H}_{\rm i}$ and $h_{\rm o}-h_{\rm i}$ are understood to be two single canonical variables conjugating respectively to the negligible $h_{\rm i}$ and $\mathcal{H}_{\rm o}$, and so they are constants that can be calculated from the initial conditions. The standard way to calculate the two negligible variables is by quadrature, after all the other degrees of freedom are integrated. But in the present context, we have as consequences of the integral of angular momentum

$$\mathcal{H}_{\rm i} + \mathcal{H}_{\rm o} = C \equiv |\boldsymbol{C}|, \quad h_{\rm o} - h_{\rm i} = \pi, \quad \mathcal{H}_{\rm o} = \frac{C^2 + \mathcal{G}_{\rm o}^2 - \mathcal{G}_{\rm i}^2}{2C}\,.$$

Therefore, only $h_{\rm i}$ needs to be calculated by quadrature. Because of the short-period terms in the integrand, computing the numerical quadrature is time-consuming. It is then preferable not to follow the standard way and only decouple $(\mathcal{H}_{\rm o}, h_{\rm o}-h_{\rm i})$ from the other degrees of freedom at this stage.

For the system defined by the Hamiltonian in Equation (1) with $h_{\rm o}-h_{\rm i}=\pi$, a first-order integrable system can be achieved by the Von Zeipel transformation (e.g. Harrington 1968, 1969; Marchal 1978, 1990). In the resulting canonical variables $(\mathcal{L}_{\rm I},\mathcal{G}_{\rm I},\mathcal{L}_{\rm O},\mathcal{G}_{\rm O},C;\ell_{\rm I},g_{\rm I},\ell_{\rm O},g_{\rm O},h_{\rm I})$, called long-period Delaunay variables, the new Hamiltonian of the first order can be written as

$$\begin{aligned}\hat{H} &= \hat{H}(\mathcal{L}_{\rm I},\mathcal{G}_{\rm I},\mathcal{L}_{\rm O},\mathcal{G}_{\rm O},C,g_{\rm I})\\ &= \hat{H}_{0{\rm I}}+\hat{H}_{0{\rm O}}+\hat{H}_1\\ &\equiv -\frac{\beta_{\rm i}}{2\mathcal{L}_{\rm I}^2}-\frac{\beta_{\rm o}}{2\mathcal{L}_{\rm O}^2}+\frac{\beta_1(3z-5)\mathcal{L}_{\rm O}}{8\mathcal{G}_{\rm O}^3}\left(\frac{\mathcal{L}_{\rm I}}{\mathcal{L}_{\rm O}}\right)^4,\end{aligned} \tag{2}$$

where

$$z=\frac{\mathcal{G}_{\rm I}^2}{\mathcal{L}_{\rm I}^2}\left[2-\left(\frac{C^2-\mathcal{G}_{\rm I}^2-\mathcal{G}_{\rm O}^2}{2\mathcal{G}_{\rm I}\mathcal{G}_{\rm O}}\right)^2\right]+5\left(1-\frac{\mathcal{G}_{\rm I}^2}{\mathcal{L}_{\rm I}^2}\right)\left[1-\left(\frac{C^2-\mathcal{G}_{\rm I}^2-\mathcal{G}_{\rm O}^2}{2\mathcal{G}_{\rm I}\mathcal{G}_{\rm O}}\right)^2\right]\sin^2 g_{\rm I}\,. \tag{3}$$

In this time-independent Hamiltonian with five degrees of freedom, there are four negligible variables $\ell_{\rm I},\ell_{\rm O},g_{\rm O}$ and $h_{\rm I}$. Their conjugate variables $\mathcal{L}_{\rm I}$, $\mathcal{L}_{\rm O}$, $\mathcal{G}_{\rm O}$ and C, together with the total energy $\hat{H}$ and $z=z(\hat{H},\mathcal{L}_{\rm I},\mathcal{L}_{\rm O},\mathcal{G}_{\rm O})$ as given by solving Equation (2), are constants known from initial conditions. This confirms the integrability of the transformed Hamiltonian system.

The differential equations for $\mathcal{G}_{\rm I}$ and $g_{\rm I}$, the variables corresponding to the only non-negligible degrees of freedom, can be integrated simultaneously. But to be more efficient, we first integrate the equation for $\mathcal{G}_{\rm I}$, decoupled from $g_{\rm I}$, by using Equation (3). In terms of $x=\frac{\mathcal{G}_{\rm I}^2}{\mathcal{L}_{\rm I}^2}\in(0,1)$, this equation can be written as

$$\dot{x}=\pm\frac{3}{2}\frac{\beta_1\mathcal{L}_{\rm I}^4}{\mathcal{L}_{\rm O}^3\mathcal{G}_{\rm O}^3}\sqrt{P_1(x)P_2(x)}\,, \tag{4}$$

where, with $A=\frac{C^2-\mathcal{G}_{\rm O}^2}{2\mathcal{G}_{\rm O}\mathcal{L}_{\rm I}}$ and $B=\frac{\mathcal{L}_{\rm I}}{2\mathcal{G}_{\rm O}}$,

$$\begin{aligned}P_1(x)&=B^2x^2-2(1+AB)x+z+A^2,\\ P_2(x)&=4B^2x^3-(5B^2+8AB+3)x^2+(4A^2+10AB-z+5)x-5A^2\,.\end{aligned}$$

From the necessary condition $P_1(x)P_2(x)\geq 0$, Marchal (1990) pointed out that x oscillates between two neighboring roots, $x_a\in(0,1)$ and $x_b\in(x_a,1)$, of $P_1(x)P_2(x)$. To be specific, the function $\dot{x}(t)$ defined in Equation (4) changes its sign from negative to positive at x_a, and the opposite is true at x_b.

The difficulty in integrating Equation (4) caused by this unfavorable feature of the right-hand side can be avoided. For this, we introduce a continuously changing angular variable θ, for which $\mathrm{mod}(2\pi)$ is not allowed, by the following variable substitution: $x=x_a+(x_b-x_a)\sin^2\theta$.

Let $\sigma_3,\sigma_4,\sigma_5$ be the other three roots of $P_1(x)P_2(x)$. We have

$$\frac{{\rm d}\tau}{{\rm d}\theta}=\mathcal{I}_1(\theta)\equiv\frac{1}{\sqrt{1-c_1\sin^2(\theta)+c_2\sin^4(\theta)-c_3\sin^6(\theta)}}\,, \tag{5}$$

where

$$\begin{aligned}\tau &= \frac{3}{4}\frac{\beta_1\mathcal{L}_{\rm I}^4}{\mathcal{L}_{\rm O}^3\mathcal{G}_{\rm O}^4}B\sigma\cdot t\,, \qquad \sigma=\sqrt{(\sigma_3-x_a)(\sigma_4-x_a)(\sigma_5-x_a)}>0\,,\\ c_1 &= d_1+d_2+d_3, \qquad c_2=d_1d_2+d_1d_3+d_2d_3,\\ c_3 &= d_1d_2d_3>0, \qquad d_j=\frac{x_b-x_a}{\sigma_{j+2}-x_a},(j=1,2,3).\end{aligned}$$

Given the initial condition (t_0, θ_0), the value of θ at any time t can be obtained from an iterative method. Also given θ, $\mathcal{G}_{\rm I}(>0)$ can be calculated from the defining formulae of θ and x.

As $|\sin g_{\rm I}(t)|$ can be solved from Equation (3), the key to determining $g_{\rm I}$ is its quadrant. Let n be the biggest integer no greater than $2\theta/\pi$. The quadrant of $g_{\rm I}(t)$ can be calculated, according to the type of motion and the values of $g_{\rm I}(0)$ and θ. Depending on the initial conditions, there are three types of motion.

Type 1: $P_2(x_a) = 0$ and $P_2(x_b) = 0$. In this type of motion, $g_{\rm I}$ oscillates around $\frac{\pi}{2}$ or $-\frac{\pi}{2}$ periodically. In the case of $\sin(g_{\rm I}(0)) > 0$, $g_{\rm I}(t)$ is in the first quadrant if n is odd and the second quadrant if n is even. In the other case, $g_{\rm I}(t)$ is in the third quadrant if n is odd and the fourth quadrant if n is even.

Type 2: $P_2(x_a) = 0$ and $P_1(x_b) = 0$. In this case, $g_{\rm I}$ always increases as time grows. The $g_{\rm I}(t)$ is in the same quadrant as $[\hat{\theta}_n, \hat{\theta}_n + \frac{\pi}{2})$, where $\hat{\theta}_n = \frac{(n-1)\pi}{2}$ if $g_{\rm I}(0)$ is in the same quadrant as $[-\frac{\pi}{2}, \frac{\pi}{2})$, and $\hat{\theta}_n = \frac{(n+1)\pi}{2}$ if $g_{\rm I}(0)$ is in the same quadrant as $[\frac{\pi}{2}, \frac{3\pi}{2})$.

Type 3: $P_1(x_a) = 0$ and $P_2(x_b) = 0$. The $g_{\rm I}$ always decreases as time goes by. The $g_{\rm I}(t)$ is in the same quadrant as $(\hat{\theta}_n - \frac{\pi}{2}, \hat{\theta}_n]$, where $\hat{\theta}_n = \left(1 - \frac{n}{2}\right)\pi$ if $g_{\rm I}(0)$ is in the same quadrant as $(0, \pi]$, and $\hat{\theta}_n = -\frac{n\pi}{2}$ if $g_{\rm I}(0)$ is in the same quadrant as $(-\pi, 0]$.

The other four angular variables can be obtained by quadrature,

$$\begin{aligned}
\ell_{\rm I}(t) &= \ell_{\rm I}(0) + \tfrac{\beta_{\rm i}}{\mathcal{L}_{\rm I}^3} t + \int_{\theta_0}^{\theta} F_1(x(\vartheta))\mathcal{I}_1(\vartheta)\mathrm{d}\vartheta, \qquad \ell_{\rm O}(t) = \ell_{\rm O}(0) + \tfrac{\beta_{\rm o}}{\mathcal{L}_{\rm O}^3} t + \tfrac{3}{8}\tfrac{\beta_1 \mathcal{L}_{\rm I}^4}{\mathcal{L}_{\rm O}^4 \mathcal{G}_{\rm O}^3}(5 - 3z)t\,, \\
g_{\rm O}(t) &= g_{\rm O}(0) + \int_{\theta_0}^{\theta} F_2(x(\vartheta))\mathcal{I}_1(\vartheta)\mathrm{d}\vartheta, \qquad\qquad h_{\rm I}(t) = h_{\rm I}(0) + \int_{\theta_0}^{\theta} F_3(x(\vartheta))\mathcal{I}_1(\vartheta)\mathrm{d}\vartheta\,,
\end{aligned}$$

where

$$\begin{aligned}
F_1(x) &= \tfrac{1}{B^2\sigma}\left[(z - \tfrac{5}{3}) + \tfrac{x(z-2)+(A-Bx)^2}{2(1-x)}\right], \\
F_2(x) &= \tfrac{5-3z}{2B\sigma} + \tfrac{1}{2B^2\sigma}\tfrac{(z-x)(A-Bx)}{x-(A-Bx)^2}\left[1 + 2B(A - Bx)\right], \\
F_3(x) &= -\tfrac{1}{2B^2\sigma}\tfrac{C}{\mathcal{G}_{\rm O}}\tfrac{(z-x)(A-Bx)}{x-(A-Bx)^2}\,.
\end{aligned}$$

If the first-order long-period solution is obtained, one can make inverse transformations of the solution to the original coordinate system.

3 COMPARISON BETWEEN M-MODEL AND K-MODEL

In order to compare the accuracy of different models in calculating the observational quantities, it is necessary to do a numerical experiment. For the time being, we are only interested in the systems with negligible 2nd-order perturbations. Therefore we generated 1000 systems, which satisfy $|H_2|/|H_{0\rm i} + H_{0\rm o} + H_1| < 0.01$ in $[-100, 100]$ years, and H_2 is the second-order perturbation term in the Hamiltonian defined in Equation (1). This time span is used because the practical cycle of a star catalog is usually less than one hundred years. As expected, for some of the generated systems, especially for the systems with large periods and high eccentricities in their outer orbits, the first-order averaged perturbations are too large. For such a case, M-model fails to be the first-order model. We only consider the samples that satisfy

$$|H_1/H_{0\rm i}| < 0.1, \quad |H_1/H_{0\rm o}| < 0.5\,, \tag{6}$$

during $[-P_t, P_t]$ years, where $P_t \geq \max(100, P_{\rm o})$, and $P_{\rm o}$ represents the initial period of the outer orbit. Nearly 90 samples are excluded by the condition stated in Equation (6). In addition, Delaunay elements are not effective in describing the orbits that are nearly circular, nearly parabolic or near the reference plane, and M-model is not suitable to be used in coplanar motion. If there are very small divisors, the implicit Zeipel transformations cannot be solved by the iterative method. Another ~ 40

samples are excluded, and 870 samples remain. The remaining samples are used to do a numerical experiment to check the accuracy of M-model compared with K-model.

We calculate the positions of three bodies in the center-of-mass frame during the $[-100, 100]$ years by both the M-model and K-model. As a standard for comparison, these positions are also calculated by the numerical solution (*N-model* for short). Denote the root-mean-squared error (*RMSE*) of the 9-dimensional vectors of M-model relative to those of N-model by $d_{\rm M}$, and the RMSE of the 9-dimensional vectors of K-model relative to those of N-model by $d_{\rm K}$. When $(r/R)^3 \ll (m_1+m_2)/m_t$, generally $d_{\rm M}/d_{\rm K} \ll 1$, as shown in Figure 1.

Figure 1 shows that M-model is apparently better than K-model in terms of accuracy when the abscissa is smaller than -1.4. When the abscissa is greater than -1.4, Figure 1 reveals that for most samples the M-model is still more accurate than the K-model.

For a few samples which are in the upper-right quarter of Figure 1, the accuracy of the M-model is not as good as that of K-model. This phenomenon can be explained by the perturbations and the improper use of Delaunay elements.

There is one sample whose ordinate is apparently greater than 0.5 in Figure 1. We found that the outer orbit of this sample has a very large period and is highly eccentric. The $\max \frac{(r/R)^3}{(m_1+m_2)/m_t}$ is really small during the considered $[-100, 100]$ years, and K-model closely approximates N-model, while M-model considers the averaged perturbations which are much greater. We calculated $\max|H - \hat{H}_{0\rm i} - \hat{H}_{0\rm o} - \hat{H}_1|$ in $[-P_t, P_t]$ years and $\max|H - H_{0\rm i} - H_{0\rm o}|$ in $[-100, 100]$ years. The former is more than 1000 times larger than the latter, and this supports that M-model is not a first-order model in such cases.

As the abscissas of samples represented by squared points are not sufficiently small (bigger than -1.4), the inaccuracies caused by small divisors cannot be ignored. For some samples represented by squared points in Figure 1, the detailed reasons are complex and currently uncertain. In all, M-model is better than K-model in accuracy for $\sim 80\%$ of the samples, and can be credibly applied when the abscissa is smaller than -1.4.

4 THE APPLICATION

Simplifications of M-model can be made according to the results of the numerical experiment. In Equation (5), $x(\theta(t))$ can be solved efficiently by an approximation. Generally $\mathcal{I}_1(\vartheta)$ can be written as

$$\mathcal{I}_1(\vartheta) = \mathcal{I}_2(\vartheta) + [\mathcal{I}_1(\vartheta) - \mathcal{I}_2(\vartheta)] \ , \tag{7}$$

where $\mathcal{I}_2(\vartheta)$ can be defined as

$$\mathcal{I}_2(\vartheta) = \begin{cases} \frac{1}{\sqrt{1-c_1\sin^2\vartheta+c_2\sin^4\vartheta}}, & \text{if} \quad c_1^2-4c_2>0, 1-c_1+c_2 \gg c_3>0, c_2>0, \\ \frac{1}{\sqrt{1-c_1\sin^2\vartheta}}, & \text{if} \quad c_1^2-4c_2\le 0, 1-c_1 \gg |c_2-c_3|>0. \end{cases}$$

The formulas for calculating $\int_0^\theta \mathcal{I}_2(\vartheta){\rm d}\vartheta$ by elliptic functions can be referred to in Byrd & Friedman (1971). Similar studies which used elliptic functions can be referred to in Kozai (1962), Soderhjelm (1982) and Solovaya (2003). The remaining term $\mathcal{I}_1(\vartheta) - \mathcal{I}_2(\vartheta)$ is generally small and sometimes can be ignored. If $\mathcal{I}_1(\vartheta) - \mathcal{I}_2(\vartheta)$ can be ignored, θ can be calculated analytically by elliptic functions. However, here $\int_{\theta_0}^{\theta} [\mathcal{I}_1(\vartheta) - \mathcal{I}_2(\vartheta)]\,{\rm d}\vartheta$ is considered by applying a simple Newton-Cotes integration formula to make a better approximation. θ can be solved approximately by an iterative method. The three angular variables $\ell_{\rm I}, g_{\rm O}, h_{\rm I}$ can also be integrated simultaneously by a simple Newton-Cotes integration formula. Another simplification is that the implicit Zeipel transformations from the averaged variables to the osculating elements can be turned into explicit forms. We call this model the MC-model.

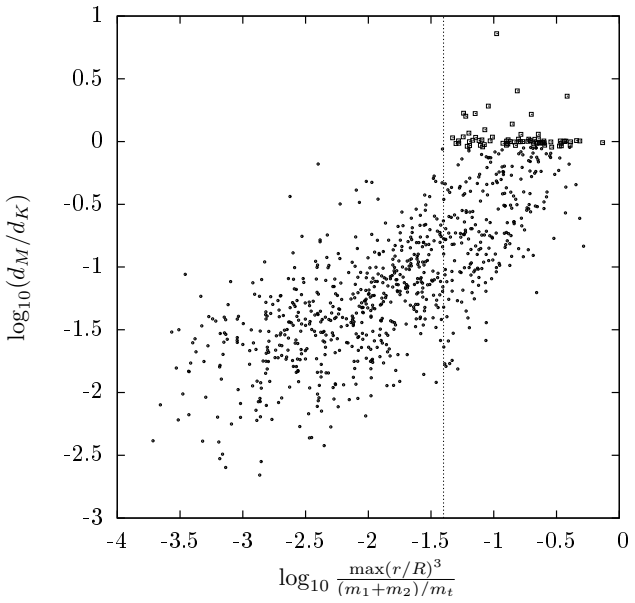

Fig. 1 The abscissas on the x-axis are calculated in $[-P_t, P_t]$ years. The abscissa of the dashed line is -1.4. Circular points represent the samples that satisfy $d_{\rm M}/d_{\rm K} < 0.9$, while square points represent the samples that satisfy $d_{\rm M}/d_{\rm K} \geq 0.9$. There are 798 circular points and 72 square points.

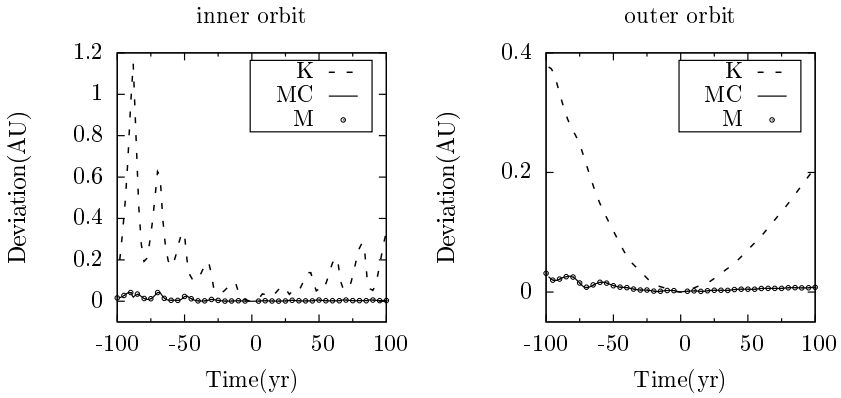

Fig. 2 From the N-model, the deviations of component positions of WDS 02022+3643 calculated separately by using M-model, MC-model and K-model.

We now apply this model to 25 real triple stars with determined dynamical states (component masses and kinematic parameters). The results are listed in Table 1, including the system name, the order of magnitude of the perturbation ($\log_{10}\frac{\max[(r/R)^3]m_t}{m_1+m_2}$), the RMSEs of M-model, K-model and MC-model, the ratio of the RMSE of the MC-model to that of the K-model ($\log_{10}\frac{d_{\rm MC}}{d_{\rm K}}$) and the type of motion. According to this table, the accuracy between the M-model and MC-model is comparable. For all these stars, the RMSE of the MC-model in comparison with that of the K-model

Table 1 The Application Results of the 25 Observed Triple Stars during the Time Span from 1900.0 to 2100.0

System name (WDS)	Perturbation order $\left(\log_{10}\frac{\max[(r/R)^3]m_t}{m_1+m_2}\right)$	$d_{\rm M}$ (AU)	$d_{\rm MC}$ (AU)	$d_{\rm K}$ (AU)	Improvement $\left(\log_{10}\frac{d_{\rm MC}}{d_{\rm K}}\right)$	Type (1/2)
00325+6714	–1.52	2.77×10^{-2}	2.78×10^{-2}	0.47	–1.23	2
01148+6056	–4.64	6.11×10^{-7}	4.96×10^{-4}	1.96×10^{-3}	–0.59	1
02022+3643	–1.56	0.013	0.013	0.23	–1.25	1
03082+4057	–4.36	7.05×10^{-4}	1.43×10^{-2}	8.32×10^{-2}	–0.76	2
04142+2812	–4.13	4.78×10^{-5}	1.10×10^{-4}	0.10	–2.96	1
04400+5328	–1.53	0.119	0.119	0.96	–0.91	2
06262+1845	–7.69	2.13×10^{-7}	2.63×10^{-6}	6.01×10^{-5}	–1.36	2
07201+2159	–7.35	7.71×10^{-9}	7.58×10^{-7}	1.23×10^{-5}	–1.21	2
10373–4814	–2.88	2.60×10^{-4}	2.41×10^{-3}	2.72×10^{-2}	–1.05	2
10373–4814	–2.77	3.49×10^{-4}	4.73×10^{-3}	3.60×10^{-2}	–0.88	2
11308+4117	–6.22	1.23×10^{-7}	4.96×10^{-6}	4.06×10^{-4}	–1.91	2
12108+3953	–1.64	0.180	0.180	0.99	–0.74	2
12199–0040	–3.24	1.31×10^{-3}	3.26×10^{-3}	0.18	–1.74	2
15183+2650	–1.76	0.014	0.014	0.12	–0.93	2
16578+4722	–2.39	6.97×10^{-4}	8.63×10^{-4}	1.66×10^{-3}	–0.28	2
17539–3445	–7.14	4.58×10^{-7}	2.47×10^{-5}	9.87×10^{-5}	–0.60	2
19155–2515	–4.08	2.06×10^{-5}	2.03×10^{-4}	1.89×10^{-2}	–1.97	1
20396+0458	–1.45	7.17×10^{-2}	7.17×10^{-2}	1.30	–1.26	1
20475+3629	–2.15	1.19×10^{-3}	1.19×10^{-3}	5.27×10^{-2}	–1.65	2
22038+6437	–5.52	4.26×10^{-7}	4.91×10^{-5}	1.40×10^{-4}	–0.46	2
22288–0001	–4.03	2.95×10^{-4}	3.32×10^{-4}	2.44×10^{-2}	–1.87	2
22388+4419	–1.86	1.94×10^{-2}	1.94×10^{-2}	0.77	–1.60	2
23078+7523	–3.98	8.76×10^{-6}	1.18×10^{-5}	2.08×10^{-3}	–2.25	2
23393+4543	–1.77	5.05×10^{-2}	5.08×10^{-2}	0.72	–1.15	2
23393+4543	–1.86	5.53×10^{-2}	5.53×10^{-2}	0.45	–0.91	2

is reduced significantly. Indeed, for $\sim 60\%$ of stars, the RMSEs are reduced by more than one order of magnitude. To show more details, we take WDS 02022+3643 as an example. From the N-model, the deviations of component positions calculated by M-model, MC-model and K-model are all shown in Figure 2. From this figure, we know that the performance of the MC-model is almost as good as that of the M-model. When compared with K-model, the model accuracy is significantly improved and the applicable time span is significantly increased.

As is well known, one of the important factors deciding the quality of dynamical state determination is the accuracy of the dynamical model. In order to show the improvement in this respect brought by the highly accurate MC-model, we apply both this model and the K-model to two systems, WDS 20396+0458 (HIP 101955, type 1) and WDS 00325+6714 (HIP 2552, type 2).

Two kinds of observations, relative position data (RPD) and the Hipparcos Intermediate Astrometric Data (HIAD), are used in the fitting. RPD are extracted from the Washington Double Star (WDS) Catalog (Mason et al. 2001), and the Fourth Catalog of Interferometric Measurements of Binary Stars (Hartkopf et al. 2001). HIAD are the abscissa residuals with respect to a reference point, the abscissa of which is calculated from a given solution. HIAD are read from the "resrec" folder in the catalog DVD of van Leeuwen (2007). With these observational data, the maximum likelihood estimate of model parameters is obtained by minimizing the objective function (χ^2)

$$\chi^2 \equiv \sum_{i=1}^{N}\left(\frac{y_{\rm i}-y(x_{\rm i};a_1\cdots a_{\rm M})}{\sigma_{\rm i}}\right)^2, \tag{8}$$

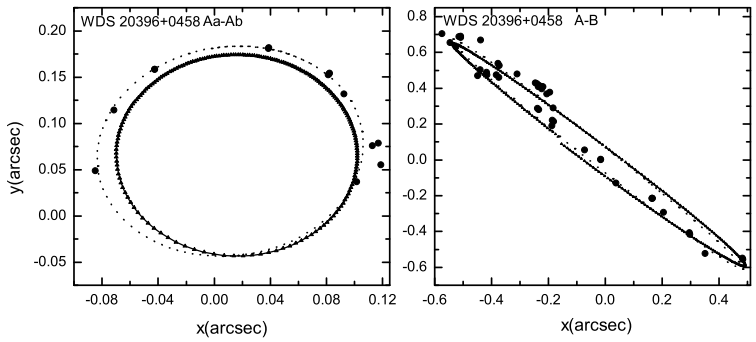

Fig. 3 The fitting result of HIP 101955.

where $y_{\rm i}$ is the observational quantity and $y(x_{\rm i}; a_1 \cdots a_{\rm M})$ is the corresponding calculated value according to the model parameters $a_1 \cdots a_{\rm M}$. We use the Bounded Variable Least Squares (BVLS) algorithm (Lawson & Hanson 1995) to minimize χ^2.

HIP 101955 is a nearby low-mass triple star. There are 15 RPD points spanning the range from 1998 to 2008 for the inner orbit, 46 points from 1934 to 2008 for the outer one, and 91 HIAD that rely on a solution with five parameters. In the previous determinations of the dynamical state, Kepler's two-body motion model is applied separately to the inner $\{Aa, Ab\}$ and the outer $\{Am, B\}$ where Am is the center-of-mass of the inner binary AaAb (Malogolovets et al. 2007). The results are collected in the *Sixth Catalog of Orbits of Visual Binary Stars* (ORB6)[2], where the inner and outer orbits are roughly evaluated as good and reliable, respectively, according to the orbital coverage of the observations. Because more observations are added, we first also use the K-model to fit observations. In comparison with the previous results, the χ^2 is found to be reduced by $\sim 66\%$. When the fitting model is replaced by the MC-model, the χ^2 is further reduced by $\sim 44\%$. Therefore, we conclude that when using the highly accurate MC-model, the fitting result is significantly better than the previous K-model's results. Using the fitted dynamical state parameters, the RMSEs of MC-model and K-model are calculated during the following 100 years, that is, from 2008 to 2108. The RMSE of MC-model in comparison with that of the K-model is significantly reduced by more than 80%, from 35.9 mas (K-model) to ~ 6.0 mas (MC-model). This result shows that although they start with the same initial conditions, for HIP 101955, the K-model cannot be used to predict the component positions.

For HIP 2552, there are 16 RPD points spanning the range from 1989 to 2005 for the inner orbit, 75 points from 1923 to 2010 for the outer one, and 151 HIAD that rely on a solution that has acceleration with seven parameters. The inner and outer orbits were provided by Docobo et al. (2008) and are evaluated as good and indeterminate respectively by ORB6. K-model is also firstly used to fit the observations. In comparison with the previous fitting results, the χ^2 is reduced by $\sim 42\%$. When the fitting model is replaced by the MC-model, though the χ^2 is not significantly reduced, the RMSE is reduced from 10.5 mas which is calculated by the K-model to 0.74 mas by the MC-model. Using the fitted dynamical parameters, during the following 100 years after the year 2010, the RMSE of K-model is 51.8 mas while that of MC-model is ~ 7.6 mas. Therefore, K-model is also not suitable for predicting the component positions of HIP 2552.

We plot the fitted trajectories of HIP 101955 and HIP 2552, respectively, in Figure 3 and Figure 4. In these two figures, the filled circles are the RPD used in the fitting, dotted curves represent the previous double two-body model while the solid curves are the fitted trajectories calculated

[2] *http://www.usno.navy.mil/USNO/astrometry/optical-IR-prod/wds/orb6*

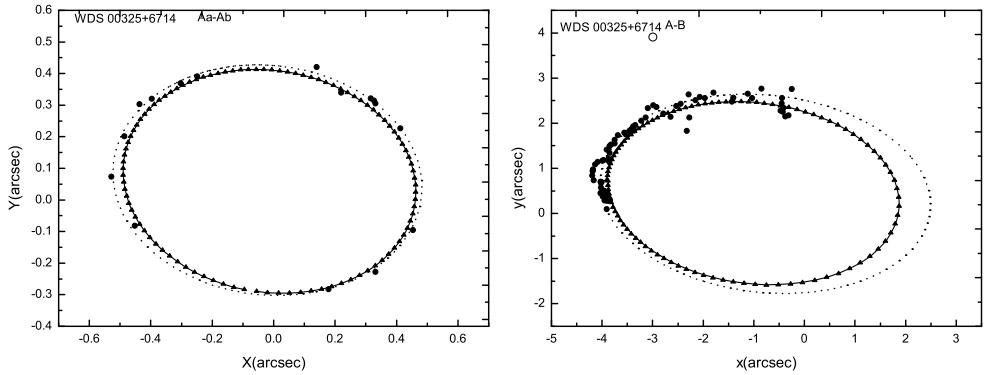

Fig. 4 The fitting result of HIP 2552. The open circle is a discarded point.

using the MC-model. The trigonometric curves represent the N-model. As shown in the two figures, the difference between the MC-model and the N-model is small enough to be ignored. The fitted dynamical state parameters and their 1σ errors are listed in Tables 2 and 3.

Table 2 The Fitted Dynamical Masses and Kinematic Parameters of HIP 101955

Parameter				Unit
$\boldsymbol{M}$	0.786±0.11	0.493±0.11	0.516±0.21	$M_\odot$
$\boldsymbol{r}_{Ab}$	–0.0598±0.0050	0.127±0.0050	–0.0188±0.022	arcsec
$\boldsymbol{r}_B$	–0.188±0.0040	0.173±0.0038	0.902±0.025	arcsec
$\boldsymbol{v}_{Ab}$	–0.102±0.0062	–0.206±0.016	0.111±0.039	arcsec yr^{-1}
$\boldsymbol{v}_B$	0.0367±0.0027	–0.174±0.0066	0.0669±0.016	arcsec yr^{-1}

Table 3 The Fitted Dynamical Masses and Kinematic Parameters of HIP 2552

Parameter				Unit
$\boldsymbol{M}$	0.389±0.038	0.0969±0.038	0.177±0.212	$M_\odot$
$\boldsymbol{r}_{Ab}$	–0.0614±0.047	–0.298±0.029	0.290±0.032	arcsec
$\boldsymbol{r}_B$	–4.029±0.016	0.609±0.015	–0.318±1.8	arcsec
$\boldsymbol{v}_{Ab}$	0.235±0.015	–0.0331±0.013	0.000668±0.025	arcsec yr^{-1}
$\boldsymbol{v}_B$	0.0478±0.0059	–0.0556±0.0029	0.0455±0.0097	arcsec yr^{-1}

5 CONCLUSIONS AND DISCUSSION

Marchal's first-order analytical solution is implemented and a more efficient simplified version is applied to real hierarchical triple stars. The results show that the proposed first-order model is preferable to the classical double two-body model both in fitting observational data and in predicting component positions.

As pointed out in Section 3, there are a few cases to which the M-model does not apply, because of the inadequacy of the Delaunay elements. For these cases, Poincaré elements should be used instead. There are also a few cases when the first-order perturbations are very small in the time span of observations, but their maximum values over the whole periods of the outer orbits are too large to apply M-model. For these cases, our preliminary studies show that it is possible to give a suitable first-order solution without resorting to averaging over the outer orbit.

Acknowledgements The authors would like to thank the reviewers of this paper for their comments and suggestions. This research is supported by the National Natural Science Foundation of China under Grant Nos. 11178006 and 11203086.

References

Aarseth, S. J. 2003, Gravitational N-Body Simulations (Cambridge: Cambridge Univ. Press)
Binney, J., & Merrifield, M. 1998, Galactic Astronomy (Princeton: Princeton Univ. Press)
Byrd, P. F., & Friedman, M. 1971, Handbook of Elliptic Integrals for Engineers and Scientists (2nd ed.; Berlin: Springer-Verlag)
Docobo, J. A., Tamazian, V. S., Balega, Y. Y., et al. 2008, A&A, 478, 187
Harrington, R. S. 1968, AJ, 73, 190
Harrington, R. S. 1969, Celestial Mechanics, 1, 200
Hartkopf, W. I., Mason, B. D., & Worley, C. E. 2001, AJ, 122, 3472
Kozai, Y. 1962, AJ, 67, 591
Lawson, C. L., & Hanson, R. J. 1995, Solving Least Squares Problems (2nd ed.; Philadelphia: SIAM)
Li, P. J., Fu, Y. N., & Sun, Y. S. 2009, A&A, 504, 277
Liu, H. D., Ren, S. L., Xia, F., & Fu, Y. N. 2009, Acta Astronomica Sinica, 50, 312
Malogolovets, E. V., Balega, Y. Y., & Rastegaev, D. A. 2007, Astrophysical Bulletin, 62, 111
Marchal, C. 1978, Acta Astronautica, 5, 745
Marchal, C., & Bozis, G. 1982, Celestial Mechanics, 26, 311
Marchal, C. 1990, The three-body problem (Amsterdam: Elsevier)
Mason, B. D., Wycoff, G. L., Hartkopf, W. I., Douglass, G. G., & Worley, C. E. 2001, AJ, 122, 3466
Orlov, V. V., & Zhuchkov, R. Y. 2005, Astronomy Reports, 49, 201
Soderhjelm, S. 1982, A&A, 107, 54
Solovaya, N. A. 2003, Contributions of the Astronomical Observatory Skalnate Pleso, 33, 179
Tokovinin, A. A. 1997, A&AS, 124, 75
Urban, S. E., & Seidelmann, P. K. 2014, Explanatory Supplement to the Astronomical Almanac, 531 (3rd ed.; Mill Valley: University Science Books)
Valtonen, M., & Karttunen, H. 2006, The Three-Body Problem (Cambridge: Cambridge Univ. Press)
van Leeuwen, F., ed. 2007, Astrophysics and Space Science Library, 350, Hipparcos, the New Reduction of the Raw Data (Berlin: Springer)